CRYSTAL GROWTH & DESIGN
2009
VOL. 9, NO. 2
858–862

Surfactant-Promoted Reductive Synthesis of Shape-Controlled Gold Nanostructures

Yingzhou Huang,[†] Wenzhong Wang,*[,†,‡] Hongyan Liang,[§] and Hongxing Xu*[,†,⊥]

Institute of Physics, Chinese Academy of Science, Beijing 100190, P. R. China, School of Science, Central University for Nationalities, Beijing 100081, P. R. China, School of Materials Science and Engineering, Shandong University, Jinan 250100, China, and Division of Solid State Physics, Lund University, Lund 22100, Sweden

Received May 14, 2008; Revised Manuscript Received September 27, 2008

ABSTRACT: We describe a surfactant-promoted reductive route for the shape-controlled synthesis of gold nanostructures by hydrothermal treatment of chloroauric acid in the presence of the surfactant hexadecyltrimethylammonium bromide (CTAB) without using reducing agent. The results show that the cationic surfactant CTAB provides the dual function of promoting Au^{III} reduction to Au^0 and size- and shape-controlled synthesis of the gold nanocrystals. More importantly, the benefit of the present work stems from the first report on the controlled synthesis of gold nanostructures by hydrothermal treatment of chloroauric acid in the presence of the surfactant CTAB without using reducing agent. The kinetics of the reduction could be manipulated through changes in the CTAB concentration to produce gold nanostructures with shapes ranging from three-dimensional (3D) octahedra, triangles, to two-dimensional (2D) hexagonal nanoplates in high yields. Growth of gold nanostructures in the CTAB solution with concentration was monitored by microscopic and spectroscopic techniques.

1. Introduction

Au nanostructures have been studied widely due to their unusual optical properties,[1] such as surface plasmonics, surface-enhanced Raman scattering (SERS), and numerous applications in bioimaging, biosensors, and photothermal therapy.[2−4] Preparation of Au nanostructures with a high degree of size and shape control has been one of the major research efforts in the gold nanomaterials field since the intrinsic properties of Au nanostructures have been highly dependent on the their morphologies. Therefore, many methods, mainly by chemical process, have been developed to synthesize Au nanostructures with unusual morphologies, such as rods,[5−8] wires,[9−12] belts,[13] plates,[10,14−16] prisms,[17,18] and branched multipods.[19−22] Some polyhedral Au nanocrystals, including cubes,[23,24] tetrahedra,[25] icosahedra,[25] octahedra,[26,27] decahedra,[28] and nanoplates,[29,30] have also been synthesized by a few methods, including modified polyol processes and seed-mediated methods. Modified polyol processes are promising techniques for preparing Au nanocrystals with different morphologies. However, appropriate choice of synthetic organic solvent, which acts both as a solvent and reducing agent for the reaction, is sometimes crucial to the successful synthesis of polyhedral Au nanocrystals. Although seed-mediated methods can be used to synthesize Au nanostructures with controllable shapes, a process to fabricate precursor seed is required for these methods. In addition, an aggressive chemical reducing agent such as sodium borohydride may be involved in these methods. There is therefore the need to develop environmentally sustainable alternatives to the existing methods. This means that the solvent system, surfactant, and reducing agent should be environmentally acceptable.

It is well known that surfactants are usually used as steric stabilizers and shape controllers in the solution-based synthetic processes of colloidal nanocrystals. In particular, hexadecyltrimethylammonium bromide (CTAB), an important cationic surfactant, has been widely used as a steric stabilizer and shape controller for nanocrystals due to its excellent capability to control the morphology of colloidal nanocrystals. It has been reported recently that surfactant CTAB could promote formation of metallic Cu nanoparticles on several metal oxides under hydrothermal conditions without any additive reductants.[31,32] Although surfactant CTAB is widely used as a shape controller in Au nanostructure synthesis, there are no reports on the synthesis of Au nanoparticles by the hydrothermal method in the presence of surfactant CTAB without using any reducing regent. Our recent systemic studies indicated that Au nanocrystals with well-controlled shape could be successfully synthesized by hydrothermal treatment of chloroauric acid in the presence of surfactant CTAB without using any reducing regent.

Here we present a new method for the synthesis of gold nanstructures with shapes ranging from three-dimensional (3D) octahedra, triangles, to two-dimensional (2D) hexagonal nanoplates in high yields for first time by hydrothermal treatment of $HAuCl_4$ in the presence of surfactant CTAB without any additive reductants in which the surfactant CTAB acts not only as a shape controller but also to promote formation of Au nanocrystals. The morphologies and sizes of these nanostructures could be well controlled by controlling the concentration of CTAB. The size transition, shape evolution, and microstructure of the as-prepared Au nanostructures were characterized by field-emission scanning electron microscopy (FESEM), transmission electron microscopy (TEM), high-resolution TEM (HRTEM), selected area electron diffraction, X-ray powder diffraction, and UV−vis absorption spectroscopy.

2. Experimental Section

For a typical synthesis of Au nano-octahedra, 412 mg (1.13 mmol) of hexadecyltrimethyl ammonium bromide (CTAB) was dissolved in 20 mL of distilled water (the concentration of CTAB is 56 mM) with the help of continuous magnetic stirring, and then 0.068 mL of $HAuCl_4$ solution (0.5 M) was added. The mixtures were transferred into a 50 mL autoclave, sealed, kept at 160 °C for 10 h in a furnace, and cooled to room temperature. The precipitates were collected and washed with distilled water.

* To whom correspondence should be addressed. E-mail: wzhwang@aphy.iphy.ac.cn; hongxingxu@aphy.iphy.ac.cn.
[†] Institute of Physics, Chinese Academy of Science.
[‡] Central University for Nationalities.
[§] Shandong University.
[⊥] Lund University.

10.1021/cg800500c CCC: $40.75
Published on Web 12/22/2008

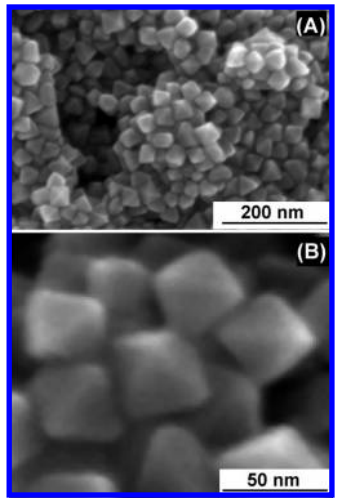

Figure 1. (A) Low- and (B) high-magnification SEM images of the as-prepared Au nano-octahedra.

Scanning electron microscopy (SEM) images were obtained using a HITACH1 S-4800 scanning electron microscope. Analysis was performed on samples deposited onto silicon supports. Transmission electron microscope (TEM) and electron diffraction studies were performed with a Philips CM-12 microscope operated at an accelerating voltage of 100 kV. Samples were prepared by dropping a dispersion of the particles in ethanol on carbon-coated copper grids. UV−vis spectroscopy was carried out on U-3010 Spectrophotometer operated at 2 nm from 900 to 250 nm.

3. Results and Discussion

It is well known that the shape of the crystals is determined by relative growth rates of particular crystallographic planes during the growth process. Here we use surfactant CTAB as a stabilizer to control the relative growth rates of different crystallographic facets and subsequently tune the morphology of Au crystals. In a typical synthesis of Au nanocrystals, 412 mg (1.13 mmol) of CTAB was dissolved in 20 mL of distilled water (the concentration of CTAB is 56 mM), and then 0.068 mL of $HAuCl_4$ solution (0.5 M) was added. The mixtures were transferred into a 50 mL autoclave, sealed, kept at 160 °C for 10 h in a furnace, and cooled to room temperature. A brownish red shining precipitate was formed. The morphology and size of the as-prepared Au nanocrystals were characterized by field-emission scanning electron microscopy (FESEM) as shown in Figure 1. Low-magnification SEM images indicate that more than 90% of the nanocrystals is regular octahedral (Figure 1A). High-magnification SEM images reveal that the surfaces of the octahedral nanocrystals are smooth with no obvious defects (Figure 1B). The average edge length of the octahedral nanocrystals is about 50 nm.

The microstructure of Au nano-octahedra was further characterized by TEM and HRTEM as shown in Figure 2. Low- and high-magnification TEM images, as shown in images A and B of Figure 2, demonstrate that the samples are composed of nano-octahera. Figure 2C shows the HRTEM image of an individual Au nano-octahedron with an edge length of 50 nm. Figure 2D shows an enlarged HRTEM image taken from the area marked with a square in Figure 2C. The clear fringes indicate that the as-prepared Au nano-octahera are single crystal.

Generally, the shape and size of the crystals may be well controlled using the dependence of reduction kinetics on concentration.[33] In the present case we found that the shape and size of Au nanocrystals could be adjusted conveniently by changing the CTAB concentration while keeping the concentration of $HAuCl_4$ unchanged. Figure 3A−D shows FESEM images of Au nanocrystals obtained at different CTAB concentrations. When the concentration of CTAB is 3.5−7 mM the as-prepared Au nanocrystals are composed of mainly hexagonal nanoplates with a few triangular nanoplates. The hexagonal nanoplates have an average lateral dimension of 7 μm and an average thickness of 150 nm as shown in Figure 3A. When the concentration of CTAB is increased to 14 mM the nanoparticles are mainly composed of triangular nanoplates with some small particles. One can clearly find that the average edge length of the triangular nanoplates is decreased to 3 μm (Figure 3B). When the concentration of CTAB is further increased to 35 mM it is clear from the SEM image (Figure 3C) that the product is mainly consisted of nano-octahedra and triangular nanoplates or nanoprisms. The average lateral size of triangular nanoplates is about 100 nm. Upon further increasing the concentration of CTAB to 56 mM the product is almost composed of nano-octahedra (more than 90%) with an edge length of 50 nm as seen in Figure 3D.

Interestingly, some of the Au triangular nanoplates (nanoprisms) can stack into a three-dimensional (3D) pattern on the carbon film when the SEM sample is prepared as shown in Figure 4A. From the side view one can see that these nanoplates self-assemble into the brick-like wall illustrated in Figure 4B.

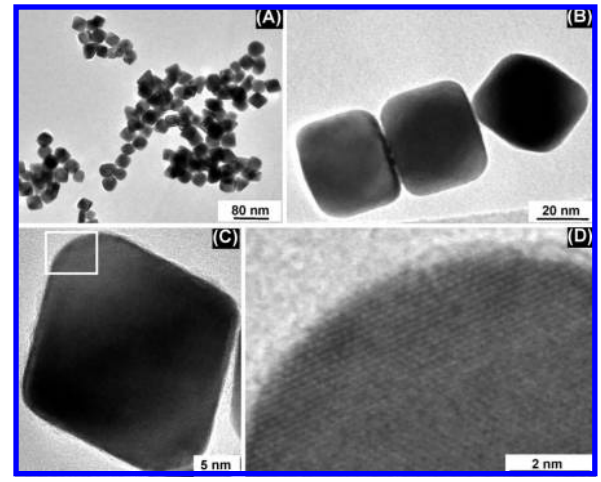

Figure 2. (A) Low- and (B) high-magnification TEM images of the as-prepared Au nano-octahedra. (C) HRTEM image of a single nano-octahedron, and (D) enlarged HRTEM image of the area in C marked with a square.

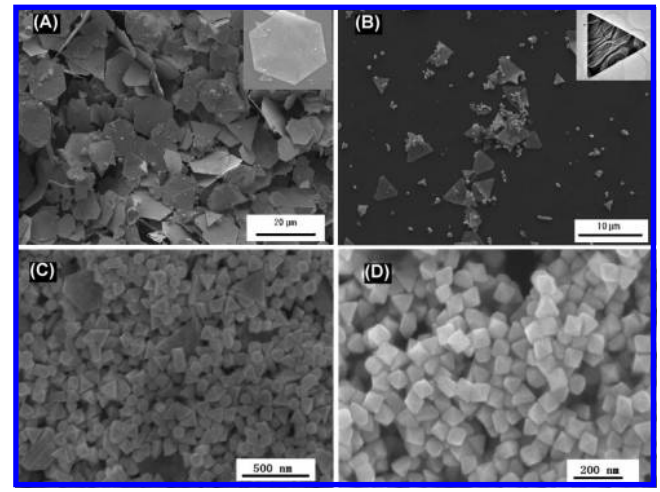

Figure 3. SEM images of Au nanostructures prepared at different CTAB concentrations: (A) 3.5, (B) 14, (C) 35, and (D) 56 mM.

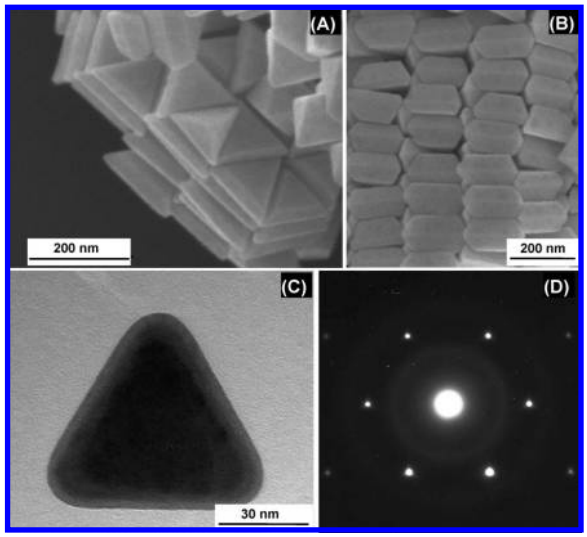

Figure 4. (A) SEM image of the Au nanoprisms with a three-dimensional (3D) pattern. (B) Side-view SEM image of the Au nanoprisms with a brick-like wall structure. (C) TEM image of a single nanoprism. (D) SAED pattern taken from a single nanoprism as shown in C.

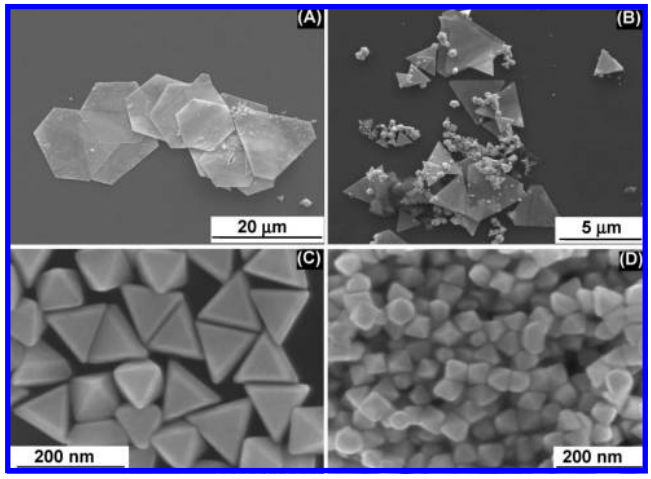

Figure 5. SEM images of Au nanostructures with different shape and size prepared at different CTAB concentrations: (A) hexagonal nanoplates with an average lateral size of 7 μm; (B) triangular nanoplates with an average of 3 μm; (C) a mixture of 53% nanoprisms and 47% nano-octahedra with an average lateral size of about 100 nm; (D) nano-octahedra with an average lateral size of about 50 nm.

The thickness of the triangular nanoplates (nanoprisms) is about 90 nm as calculated from Figure 4B. The morphology and crystallinity of triangular nanoplates (nanoprisms) are further characterized by TEM and SAED. Figure 4C shows a TEM image of an individual nanoplate, indicating that the nanoplate has a triangular shape with an equilateral of 60 nm. The SAED pattern (Figure 4D) taken from a single nanoprism (Figure 4C) indicates that the triangular nanoplates (nanoprisms) are single crystal.

The CTAB concentration was found to influence the shape and size of Au nanocrystals in three ways: First, an increase of the CTAB concentration led to a decrease in the average lateral size of the hexagonal and triangular particles. For the particles shown in Figure 5A−C the average lateral size of the nanoplates was decreased from 7 μm for that prepared at the lowest CTAB concentration (3.5−7 mM) to 100 nm prepared at a higher CTAB concentration (35 mM). The fast reduction expected at high CTAB concentrations could greatly increase the super-

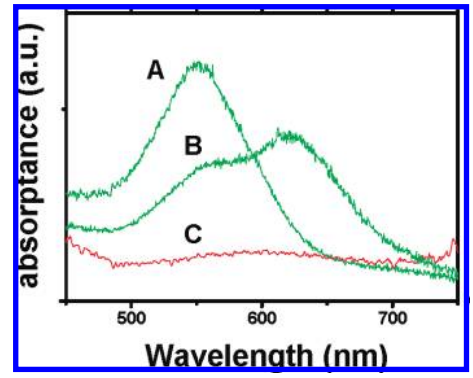

Figure 6. UV−vis absorption spectra of the Au nanocrystals prepared with different CTAB concentrations: (A) CTAB, 56 mM, nano-octahedra ≈ 90%; (B) CTAB, 40 mM, nano-octahedra ≈ 47%, nanoprisms ≈ 53%; (C) CTAB, 3.5 mM, hexagonal nanoplates).

saturation level of Au^0 in solution and subsequently the number of Au seeds formed in the nucleation step. It has been reported that an increase in the number of seeds induces formation of Au nanoplates with a smaller size during a fixed gold−precursor concentration.[15,34] Second, an increase in the CTAB concentration led to a decrease in the yield of Au nanoplates as seen in Figure 5A−C. The trend mirrors the selectivity of CTAB binding on different Au surfaces at different CTAB concentrations. The selective adsorption of CTAB molecules on the {111} planes was responsible for formation of hexagonal and triangular plates with {111} basal planes.[15,35] The selectivity of adsorption was lower at higher CTAB concentrations, and adsorption of CTAB molecules on the sides of the plates bound by {100} and/or {111} planes led to diminished anisotropic growth and consequently a poorer yield of the nanoplates.[15,35] Similar phenomena have been observed previously during the formation process of Ag nanoplates with CTAB as the shape-directing agent.[15,35] Third, The CTAB concentration strongly influenced the morphology of Au nanocrystals. As shown in Figure 5A, at a low CTAB concentration (3.5−7 mM) the concentration of hexagonal nanoplates was higher than that of triangular nanoplates, which accounted for less than 5% of the total synthesized nanoplates. At a higher CTAB concentration (14 mM) sharp triangular nanoplates were the dominant shape formed among all of the particles (Figure 5B). At a much higher CTAB concentration (35 mM) the morphology of some Au nanocrystals was dramatically changed from 2D nanoplates to 3D nano-octahedra as clearly seen in Figure 5C. In Figure 5C the concentration of the nano-octahedra was about 47%, which was lower than that of triangular nanoplates, which was about 53%. At the highest CTAB concentration (56 mM) regular nano-octahedra were the exclusive shape (more than 90%) among all the formed anisotropic particles as shown in Figure 5D.

The shape and size control of Au nanocrystals can also be witnessed by UV−vis spectroscopy studies. It has been reported that the optical properties of metal nanoparticles are strongly shape and size dependent. Small spherical Ag or Au nanocrystals displayed only a single surface plasmon resonance (SPR), whereas two or three SPR bands were expected from the anisotropic particles depending on their shape and size. Figure 6 shows the UV−vis spectra of Au nanocrystals prepared with different CTAB concentrations. There is only one SPR in the spectrum taken from the Au nano-octahedra (more than 90%) that is prepared at the highest concentration of CTAB (56 mM). The SPR is located at 570 nm (curve A), which is in agreement with that of the Au nano-octahedra with a similar size. Two SPR bands from the sample prepared with lower CTAB

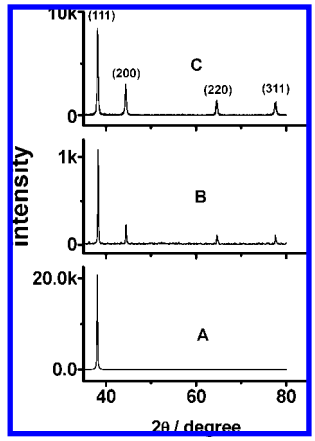

Figure 7. XRD patterns of the as-prepared Au nanocrystals: (A) hexagonal nanoplates, (B) triangular nanoplates with a few nano-octahedra, and (C) nano-octahedra.

concentration (40 mM) are clearly visible as shown in curve B of Figure 6. The curve can be fitted with two peaks centered at 570 and 630 nm by Gaussian fitting, respectively. The SPR at 570 nm comes from Au nano-octahedra with an average edge length of 50 nm as observed in the SEM images (Figure 1). A similar SPR was also observed in the Au nano-octahedra (~90%) with an average edge length of about 60 nm by Cho and co-workers.[26] The SPR at 630 nm comes from Au triangular nanoprisms of the sample. Similar SPR from the Au triangular nanoprisms with lateral dimensions of 200 nm and a height of 40 nm were observed previously.[18] The absorption spectrum for the microsized Au nanoplates, which were synthesized at the lowest CTAB concentration (3.5 mM), shows a gradual increase in absorption from 500 to 600 nm, and then the absorption increases steadily into the near-IR region (curve C in Figure 6). We cannot detect an obvious absorption peak in the spectrum of microsized Au nanoplates resulting from a mixture of nanoplate shapes over a range of sizes in the sample.

The structural information and evidence of the crystallinity of the as-prepared Au nano-octahedra and nanoplates were further investigated by powder X-ray diffraction (XRD). Figure 7 shows typical XRD patterns of the as-synthesized Au hexagonal plates, triangular plates, and octahedra. All diffraction peaks can be easily assigned to the (111), (200), (220), and (331) planes of face-centered cubic structure of gold. It is noted that all samples exhibit an extremely strong (111) diffraction peak, indicating that the Au crystals with octahedral- and plated-like shape are essentially composed of (111) lattice planes as reported before.[10,26] The XRD of the hexagonal nanoplates exhibits only the (111) peak (Figure 7A), indicating that the plates are dominant with {111} facets oriented parallel to the surface of the supporting substrate. Figure 7C shows that the intensity ratio of the (200) and (111) diffraction peaks is 0.36, which is lower than that of the bulk value of 0.53, suggesting that the nano-octahedra are abundant in {111} planes. This result indicates that {111} planes of the as-prepared Au nano-octahedra tend to preferentially orient parallel to the surface of the supporting substrate. Thus, the XRD results further provide evidence that selective adsorption of CTAB molecules on the {111} planes was responsible for formation of hexagonal, triangular plates and octahedra with {111} basal planes.

The experimental results indicated that the temperature also played an important role in formation of Au nanocrystals under hydrothermal treatment of $HAuCl_4$ in the presence of surfactant CTAB without any additive reductants. The color change of the solution, containing the same concentration of CTAB and

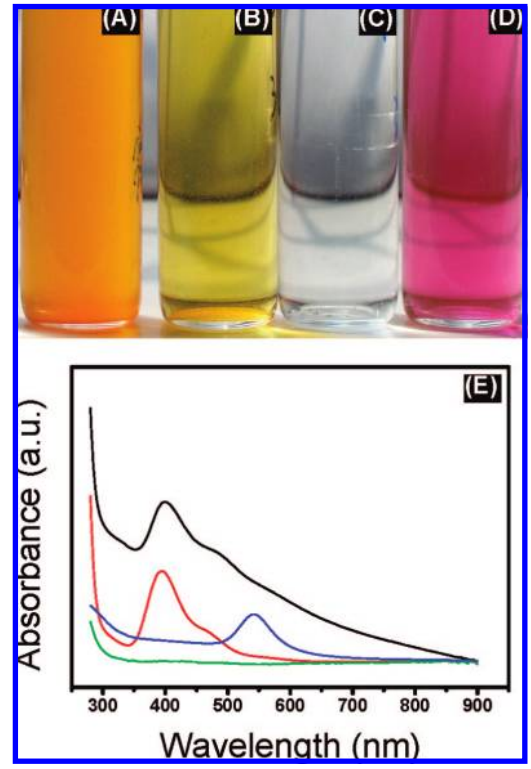

Figure 8. Color of the solution prepared at different temperatures: (A) room temperature, (B) 100 °C, (C) 130 °C, and (D) 160 °C. (E) Corresponding UV−vis spectra of the as-prepared solution: (black line) room temperature; (red line) 100 °C; (green line) 130 °C; (blue line) 160 °C.

Au^{3+}, prepared at different temperatures and their corresponding UV−vis spectra give evidence of temperature for formation of Au nanocrystals as shown Figure 8. At room temperature the color of the 50 mL solution containing 412 mg (1.13 mmol) of CTAB and 0.068 mL of $HAuCl_4$ solution (0.5 M) is yellow as shown in Figure 8A. Its corresponding UV−vis spectrum is shown in Figure 8E (black line) in which a characteristic absorption peak at 400 nm is observed. The absorption is attributed to tetrabromo aurate ions, which is in good agreement with the experimental data of Mortier et al.[36] When the solution was heated in an autoclave at 100 °C for 10 h its color was still yellow (buff) as shown in Figure 8B. The corresponding UV−vis spectrum also exhibits a characteristic absorption band of tetrabromo aurate ions as seen in Figure 8E (red line). However, when the solution was heated in an autoclave at 130 °C for 10 h its color changed from yellow to colorless (Figure 8C). The characteristic absorption peak of tetrabromo aurate ions also completely disappears as shown by the green line of Figure 8E. A similar phenomenon was observed by Mortier et al.[36] They attributed it to formation of another gold ion, $AuBr^{2-}$, $AuBr^{2-}$ being a colorless compound.[37,38] When the solution was heated higher than 160 °C in an autoclave for 10 h its color changed from yellow to brownish red (Figure 8D); the corresponding UV−vis absorption spectrum clearly exhibits an absorption peak at 560 nm as shown in Figure 8E (blue line), indicating formation of Au nanocrystals.

The color change and corresponding UV−vis spectra (Figure 8) could give us a rational explanation for reducing Au^{III} to Au^0 during the hydrothermal process in the presence of CTAB without reducing agent. At room temperature and/or below 100 °C the interaction between $HAuCl_4$ and CTAB produces the tetrabromo aurate ions (Figure 8A, 8B, and 8E). A trace amount of NH_3/NH_4OH may be produced in this process. When

temperature is increased to 130 °C $AuBr^{2-}$ is produced by interaction between $HAuCl_4$ and CTAB (Figure 8C and 8E). This process may also produce a trace amount of NH_3/NH_4OH. When the temperature is above 160 °C Au^{III} is reduced to Au^0, and finally, the Au nanocrystals are formed from nucleation and aggregation of Au^0. Meanwhile, it has been reported recently that CTAB decomposes to NH_3/NH_4OH under hydrothermal conditions at about 160 °C,[31,32] and the Au precursor ($HAuCl_4$, tetrabromo aurate ions, and $AuBr^{2-}$) may enhance decomposition of CTAB to NH_3/NH_4OH,[39] which may reduce the Au^{III} species to the metallic Au^0 state under hydrothermal conditions at above 160 °C. This is reason that we cannot obtain Au nanocrystals when the heating temperature is lower than 160 °C.

The above experimental results indicate that the surfactant CTAB plays a key role in formation of Au nanostructure. Previous studies revealed that surfactant CTAB could act not only as a stabilizer to prevent aggregation of the crystals but also as a shape controller to assist formation of anisotropic metal nanostructures. In the present case, CTAB not only acts as a stabilizer and a shape controller for formation of anisotropic Au nanostructures but also promotes reduction of Au^{III} to Au^0 under hydrothermal conditions. A possible growth process of Au nanostructures could be concluded as follows. At the initial stage the dominant process is formation of tiny Au crystal nuclei, which is formed by CTAB promoting. With increasing time, these tiny nuclei, fixed by CTAB molecules, coalescence with adjacent ones, decreasing their surface energy and enhancing formation of different shapes of nanocrystals because the binding between CTAB and Au inhibits crystal growth randomly and favors growth with their different preferred facets at different concentrations. At a low concentration of CTAB the effect of selective adsorption of CTAB molecules on Au crystal faces induces higher nanocrystal surface coverage and favors production of discal Au nanocrystals. Once discal Au nanocrystals are formed they serve as "seeds" to further grow into Au plates via a seed-medicated approach because of minimization of energy. The low concentration of CTAB results in not so many nuclei formed at a time. It enhances the possibility for the nanoplates to grow slowly to micrometer size. Selective adsorption of CTAB molecules on the {111} planes was responsible for formation of hexagonal and triangular plates with {111} basal planes.[15,35] The selectivity of adsorption was lower at higher CTAB concentrations, and adsorption of CTAB molecules on the sides of the plates bound by {100} and/or {111} planes led to diminished anisotropic growth and consequently a poorer yield of the nanoplates.[15,35] As the concentration of CTAB increases to the highest level the fast reduced nuclei prefer to form a large-scale octahedral seeds, leading to a high yield of nano-octahedra with uniform size. Analysis indicates that growth of the Au nanocrystal involves the self-seeding and seeding growth process. Another possible growth process of the Au triangular and hexagonal plates may be due to a simple well-known nucleation and oriented growth process.

4. Conclusions

In summary, we demonstrated a hydrothermal route which is simple, convenient, economical, and environmentally benign using the CTAB not only as a shape controller but also as promoting formation of Au nanocrystals for the synthesis and shape modulation of the highly pure Au nanostructure in high yield. The shapes and size of the Au nanostructure are modulated by the concentration of CTAB remaining under the same conditions. The as-prepared Au nanostructures exhibit attractive optical properties. Both the Au nanostructure with high purity and the synthesis route demonstrated here have expanded the ability to further study the unique optical properties and applications of Au nanostructures. This method opens a new avenue for the shape-controlled synthesis of gold nanostructures.

References

(1) (a) Cao, Y. W.; Jin, R. C.; Mirkin, C. A. *Science* **2002**, *297*, 1356–1540. (b) Burda, C.; Chen, X. B.; Narayanan, R.; El-Sayed, M. A. *Chem. Rev.* **2005**, *105*, 1025–1102. (c) Rosi, N. L.; Mirkin, C. A. *Chem. Rev.* **2005**, *105*, 1547–1562.
(2) Huang, X. H.; El-Sayed, I. H.; Qian, W.; El-Sayed, M. A. *J. Am. Chem. Soc.* **2006**, *128*, 2115–2120.
(3) Li, C.-Z.; Male, K. B.; Hrapovic, S. T.; Luong, J. H. *Chem. Commun.* **2005**, *392*, 4–3926.
(4) Sudeep, P. K.; Joseph, S. T. S.; Thomas, K. G. *J. Am. Chem. Soc.* **2005**, *127*, 6516–6517.
(5) Kim, F.; Song, J. H.; Yang, P. *J. Am. Chem. Soc.* **2002**, *124*, 14316–14317.
(6) Zweifel, D. A. *Chem. Mater.* **2005**, *17*, 4256–4261.
(7) Sau, T. K.; Murphy, C. J. *Langmuir* **2004**, *20*, 6414–6418.
(8) Nikoobakht, B.; El-Sayed, M. A. *Chem. Mater.* **2003**, *15*, 1957–1962.
(9) Tosatti, E.; Prestipino, S. *Science* **2000**, *289*, 561–563.
(10) Liu, X. G.; Wu, N. Q.; Wunsch, B. H.; Barsotti, R. J.; Stellacci, F. *Small* **2006**, *2*, 1046–1050.
(11) Sainsbury, T.; Fitzmaurice, D. *Chem. Mater.* **2004**, *16*, 2174–2179.
(12) Hutchinson, T. O.; Liu, Y. P.; Kiely, C.; Brust, M. *Adv. Mater.* **2001**, *13*, 1800–1803.
(13) Zhang, J. L.; Du, J. M.; Han, B. X.; Liu, Z. M.; Jiang, T.; Zhang, Z. F. *Angew. Chem., Int. Ed.* **2006**, *45*, 1116–1119.
(14) Sun, X.; Dong, S.; Wang, E. *Angew. Chem., Int. Ed.* **2004**, *43*, 6360–6363.
(15) Xie, J.; Lee, J. Y.; Wang, D. I. C.; Ting, Y. P. *Small* **2007**, *3*, 672–682.
(16) Brohm, D.; Metzger, S.; Bhargava, A.; Muller, O.; Lieb, F.; Waldmann, H. *Angew. Chem., Int. Ed.* **2002**, *41*, 195–199.
(17) Shankar, S. S.; Rai, A.; Ankamwar, B.; Singh, A.; Ahmad, A.; Sastry, M. *Nat. Mater.* **2004**, *3*, 482–488.
(18) Pompa, P. P.; Martiraddonna, L.; Torre, A. D.; Salla, F. D.; Manna, L.; Vittorio, M. D.; Calabi, F.; Cingolani, R.; Rinaldi, R. *Nat. Nanotechnol.* **2006**, *1*, 126–130.
(19) Sau, T. K.; Murphy, C. J. *J. Am. Chem. Soc.* **2004**, *126*, 8648–8649.
(20) Chen, S. H.; Wang, Z. L.; Ballato, J.; Foulger, S. H.; Carroll, D. L. *J. Am. Chem. Soc.* **2003**, *125*, 16186–16187.
(21) Hao, E. C.; Bailey, R. C.; Schatz, G. C.; Hupp, J. T.; Li, S. Y. *Nano Lett.* **2004**, *4*, 327–330.
(22) Yamamoto, M.; Kashiwagi, Y.; Sakata, T.; Mori, H.; Nakamoto, M. *Chem. Mater.* **2005**, *11*, 5391–5393.
(23) Sun, Y. G.; Xia, Y. N. *Science* **2002**, *298*, 2176–2179.
(24) Jin, R. C.; Egusa, S. J.; Scherer, N. F. *J. Am. Chem. Soc.* **2004**, *126*, 9900–9901.
(25) Kim, F.; Connor, S.; Song, H.; Kuykendall, Y.; Yang, P. D. *Angew. Chem., Int. Ed.* **2004**, *43*, 3673–3677.
(26) Li, C.; Shuford, K. L.; Park, Q. H.; Yue, W. C.; Li, Y.; Lee, E. J.; Cho, S. O. *Angew. Chem., Int. Ed.* **2007**, *46*, 3264–3269.
(27) Zhang, J.; Gao, Y.; Puebla, R. A.; Buriak, J. M.; Fenniri, H. *Adv. Mater.* **2006**, *18*, 3233–3237.
(28) Iglesias, A. S.; Santos, I. P.; Juste, J. P.; Gonzalez, B. R.; Abajo, F. J.; Marzan, L. M. *Adv. Mater.* **2006**, *18*, 2529–2534.
(29) Sun, X.; Dong, S.; Wang, E. Angew. *Chem., Int. Ed.* **2004**, *46*, 6360–6362.
(30) Luo, Y. L. *Mater. Lett.* **2007**, *61*, 1346–1349.
(31) Bal, R.; Tada, M.; Iwasawa, Y. *Chem. Commun.* **2005**, 3433–3435.
(32) Tada, M.; Bal, R.; Namba, S.; Iwasawa, Y. *Appl. Catal. A: Gen.* **2006**, *307*, 78–84.
(33) Daniel, M. C.; Astruc, D. *Chem. Rev.* **2004**, *104*, 293–346.
(34) Brown, K. R.; Walter, D. G.; Natan, M. J. *Chem. Mater.* **2000**, *12*, 306–313.
(35) Chen, S. H.; Carroll, D. L. *J. Phys. Chem. B* **2004**, *108*, 5500–5506.
(36) Mortier, T.; Verbiest, T.; Persoons, A. *Chem. Phys. Lett.* **2003**, *382*, 650–653.
(37) Braunstein, P.; Clark, R. J. H. *J. Chem. Soc., Dalton Trans.* **1973**, 1845–1848.
(38) Savas, M.; Mason, W. R. *Inorg. Chem.* **1987**, *26*, 301–304.
(39) Shi, F.; Deng, Q.; Sima, T. L.; Gong, C. K. *Chem. J. Chin. Univ.* **2001**, *22*, 645–647.

CG800500C